Available online at www.sciencedirect.com

SCIENCE DIRECT

Remote Sensing of Environment 97 (2005) 116 – 126

Remote Sensing of Environment

www.elsevier.com/locate/rse

Satellite remote sensing classification of thaw lakes and drained thaw lake basins on the North Slope of Alaska

Robert C. Frohn*, Kenneth M. Hinkel, Wendy R. Eisner

University of Cincinnati, Department of Geography, Cincinnati, Ohio 45221-0131, United States

Received 28 December 2004; received in revised form 22 April 2005; accepted 24 April 2005

Abstract

The purpose of this research was to map thaw lakes and drained thaw lake basins (DTLBs) on the North Slope of Alaska using satellite remote sensing. This research is the first to map DTLBs on a large scale for Alaska's Arctic Coastal Plain. Thaw lakes and DTLBs were classified from seven Landsat-7 scenes using texture analysis, spectral transformations, and image segmentation. The overall classification accuracy was 97.7% with a Kappa coefficient of 0.96. Thaw lakes had a producer accuracy of 99.1% and a user accuracy of 98.6%, while DTLBs had a producer accuracy of 93.8% and user accuracy of 98.1%. A total of 7054 km^2 of thaw lakes were mapped, accounting for 20.4% of the Arctic Coastal Plain; there were 8917 km^2 of DTLBs covering 25.7% of the study area. Continued research in the analysis of thaw lakes and DTLBs is crucial to our understanding of the global carbon cycle, atmospheric methane concentrations, heat flow and climate change.

Keywords: Image segmentation; Thaw lakes; Drained thaw lake basins; Alaska; Arctic Coastal Plain

1. Introduction

The North Slope of Alaska is characterized by thousands of thaw lakes and drained thaw lake basins (DTLBs) developed atop continuous permafrost. Thaw lakes cover from 20% to as much as 40% of the Alaskan Arctic Coastal Plain, and large portions of the Arctic Foothills and Seward Peninsula (Black, 1969; Livingstone et al., 1958; Sellmann et al., 1975a). Many thaw lakes are oriented with the long axis of the elliptical lake at 10°–20° west of geographic north and nearly perpendicular to the prevailing wind direction (Sellmann et al., 1975a). Lake size is a function of ground ice volume, local and regional relief, and age (Sellmann et al., 1975a). In winter, the heat flow from these lakes is similar to that of the nearby Arctic Ocean (Jeffries et al., 1999; Kozlenko & Jeffries, 2000). In spring, the ice cover melts and lakes contribute a significant pulse of methane to the atmosphere (Phelps et al., 1998). Thaw lakes are an important natural resource for floral and faunal communities and provide water for public and industrial use (Mellor, 1994).

Thaw lakes are a primary mechanism of landscape modification as they slowly grow in size, coalesce with other lakes, migrate across the landscape, and often rapidly drain (Kozlenko & Jeffries, 2000). The depressions formerly occupied by thaw lakes are known as drained thaw lake basins. Hussey and Michaelson (1966) estimated that 50–75% of the Arctic Coastal Plain is covered either by lakes or by mires in former thaw-lake basins. DTLBs are sites for the preferential accumulation of soil organic carbon in the form of peat, and Arctic peatlands have global significance as sources of CO_2 and CH_4. An increase in the average depth of the seasonal thaw layer in response to expected warming at high latitudes is of concern owing to the large quantity of soil organic carbon (SOC) sequestered in the upper permafrost that could become mobilized following enhanced soil microbial respiration (e.g., Billings et al., 1982; Christensen et al., 2004; Waelbroeck et al., 1997;

* Corresponding author. Tel.: +1 513 556 2849; fax: +1 513 556 3370.
E-mail address: robert.frohn@uc.edu (R.C. Frohn).

0034-4257/$ - see front matter © 2005 Elsevier Inc. All rights reserved.
doi:10.1016/j.rse.2005.04.022

Weller et al., 1995). The magnitude of outgasing effects is dictated by the anticipated depth of thaw and amount of sequestered carbon that would be available (Kane et al., 1992; Serreze et al., 2000). Recently, Smith et al. (2004) reported that West Siberian peatlands have likely been a long-term sink of atmospheric CO_2 but a source of CH_4. An account of the change in total greenhouse forcing or total carbon balance has yet to be completed in northern Alaska.

A model of the thaw-lake cycle was established for the Arctic Coastal Plain of northern Alaska (Britton, 1966; Billings & Peterson, 1980; Hopkins, 1949). The cycle begins with ponding over ice-wedge troughs and low-center polygons. Eventually, ponds coalesce and enlarge to form a small lake. Lake dimensions increase over time due to the combined effects of thermo-mechanical erosion of lake margins and thaw of ice-rich permafrost beneath the standing water. If the lake is sufficiently deep (>2 m), ice wedge growth will cease and the wedges may begin to ablate as the thaw bulb below the lake deepens.

Lake drainage is triggered by stream piracy, tapping, bank overflow, or ice-wedge erosion (Hopkins, 1949; Mackay, 1988; Walker, 1978). Drainage by ice-wedge erosion appears to be catastrophic (Hopkins & Kidd, 1988; Mackay, 1992); Mackay (1988) estimates that 1–2 lakes in the Tuktoyaktuk Peninsula of northwest Canada completely or partially drain suddenly each year. Revegetation and organic matter accumulation begins, and ice-wedge growth is re-activated as permafrost aggrades into the unfrozen substrate below the drained lake basin (Mackay & Burn, 2002). Eventually, ice-wedge growth yields low-centered polygons with ponds developing preferentially over the resulting troughs. In this way, a thaw-lake cycle begins again. The thaw-lake cycle was previously thought to have a duration of 2000–3000 years (Britton, 1966; Sellmann et al., 1975a), but recent investigations indicate that several basins drained prior to 5000 BP and do not appear to be redeveloping as lakes (Hinkel et al., 2003).

Following drainage, revegetation and peat accumulation begin. Successional processes are relatively slow in arctic tundra as edaphic conditions change, resulting in a mosaic of plant communities that reflects the relative age of the basin (Billings & Peterson, 1980; Bliss & Peterson, 1992; Webber, 1978). Heave, ice-wedge polygon development, and slope processes combine to slowly obliterate the basin, and it eventually appears as upland or wet meadow tundra consisting primarily of grasses and sedges. Since DTLBs often develop in older basins, the landscape is dominated by nested or overlapping patterns. This forms a palimpsest, where older landforms are progressively obliterated by younger.

2. Previous studies

Several researchers have studied thaw lakes in northern Alaska using satellite remote sensing (Frohn et al., 2001; Hinkel et al., 2003; Jeffries et al., 1996; Jeffries et al., 1999; Kozlenko & Jeffries, 2000; Mellor, 1994; Sellmann et al., 1975a,b). Sellmann (1975a) used Landsat-1 data to help categorize thaw lakes by size, axis length/width ratio, orientation, degree of basin development and lake density. Synthetic Aperture Radar (SAR) ERS-1 data has been used for estimating thaw lake depth (Jeffries et al., 1996), measuring heat flow from thaw lakes (Jeffries et al., 1999) and in bathymetric mapping of thaw lakes (Kozlenko & Jeffries, 2000). However, very little research has been done with respect to the analysis of DTLBs using satellite remote sensing. Frohn et al. (2001) and Hinkel et al. (2003) mapped lakes and DTLBs according to relative age classes on the ~1600 km^2 Barrow Peninsula using Landsat-7 data, but DTLBs have not been mapped for larger areas of the Arctic Coastal Plain. Black (1969) noted 35 years ago that thousands of DTLBs can be recognized by their surficial expression and characteristic sediments, but the economic incentive to map them was lacking.

The relative age of a DTLB can be estimated by the degree of vegetation succession as plant communities respond to changing conditions (Carson & Hussey, 1962; Eisner & Peterson, 1998; Frohn et al., 2001; Hinkel et al., 2003). The relative age of 77 DTLBs near Barrow was determined by field visits. Soil cores were taken from 21 basins; samples of peat were collected from the interface of the organic layer and underlying lacustrine mineral sediment, which marks the initiation of plant growth following lake drainage. Radiocarbon dates were used to assign absolute ages to bracket the relative categories (Hinkel et al., 2003). Analysis of hundreds of cores collected in DTLBs of varying ages demonstrates that the thickness of the organic layer increases with basin age (Bockheim et al., 2004). Since the Arctic Coastal Plain is covered by DTLBs of various ages, the spatial distribution of SOC is also highly variable.

For the studies around Barrow, DTLBs were manually digitized (Frohn et al., 2001; Hinkel et al., 2003). Using 42 basins as training samples, spectral and textural transforms were applied with pattern recognition algorithms in a neural network classification scheme. An additional 35 field-classified basins constituted a verification dataset. The spectral age classification scheme was 71% accurate in assigning basins to the proper age category. The classification algorithm was then applied to 558 DTLBs that were identified on the Barrow Peninsula. Average SOC by basin age was weighted by the basin area per age category to determine the average SOC in the study area.

For the Barrow Peninsula north of ~71° latitude, several general conclusions can be made (Hinkel et al., 2003): (1) Lake and DTLB orientation do not differ significantly; the long axis of the elliptical shape is around N 08° W across the entire range of sizes; (2) Bockheim et al. (2004) examined soils in 20 DTLBs representing an age continuum from 50 to 5500 years. In general, organic layer thickness, ice content and the degree of organic matter decomposition

increases with basin age; (3) SOC tends to increase with basin age; profile SOC pools in DTLBs average 48 kg C m^{-3}; (4) The spectral classification algorithm, applied to Landsat-7 ETM+ summer imagery, produces reasonable estimates of field-determined DTLB age; (5) Radiocarbon dating shows a reasonably strong correlation between field-based basin age classification and ^{14}C age, implying that the factors used to discriminate basin age are valid; (6) Spatially weighted estimates of SOC indicate that there are 40 kg C m^{-3} in the 78% of the area not covered by lakes; (7) About 28% of the land surface, classified as "non-basin," is actually scarred by thaw-lake processes. However, the basins are so old and overlapping that individual basins can no longer be easily discerned; and (8) There appears to be a few erosional remnants of a much older surface that have remained unaffected by the thaw lake cycle. These can be identified by their topographic prominence (>20 m), atypical plant community, high ice content and degree of ice-wedge polygon development, and spectral signature (Eisner et al., 2005). Basal core samples from one site date to ca. 9000 cal BP.

The primary limitation to this approach is the need to manually digitize DTLBs. Sellmann et al. (1975a) analyzed lake properties using Landsat-1 images and 1:250,000 USGS topographic maps. In their study of oriented lakes on the Tuktoyaktuk Peninsula in the western Arctic, Côté and Burn (2002) used Canadian National Topographic Survey digital base maps at the same scale. These sources often lack the resolution necessary to identify and capture DTLB margins across the ranges of sizes. Furthermore, because it is time consuming and highly subjective, the manual method can only be applied to small study areas. In order to extend our study to the entire Arctic Coastal Plain, our goal was to first develop an automated algorithm to recognize DTLB margins.

This paper describes the methodology used to achieve this goal. The objectives of this paper are (1) to describe the algorithms used to identify and isolate lakes and DTLBs; (2) to perform an accuracy assessment of the classification; (3) to calculate size parameters, frequency distribution, and areal extent of thaw lakes and DTLBs on the western Arctic Coastal Plain; and (4) to perform a preliminary comparison of lake and DTLB characteristics between the Outer Coastal Plain (0–23 m asl) and Inner Coastal Plain (23–120 m asl) where the age, vegetation and edaphic conditions are different. This has implications for understanding the geomorphic differences and landscape evolution of the Coastal Plain.

3. Study area

The study area is the western Arctic Coastal Plain of Alaska extending from the Colville River (152 W° longitude) to the Chukchi Sea (162° W longitude). Landward of the Coastal Plain is the Arctic Foothills physiographic province (Wahrhaftig, 1965), which are the glaciated foothills of the east–west trending Brooks Range. The study region is underlain by continuous permafrost and is characterized by tundra vegetation, low elevation and relief, oriented thaw lakes and DTLBs. The region is bisected by a number of meandering and braided streams in broad valleys.

The Coastal Plain has been subjected to several marine transgressions during the late Cenozoic (Brigham-Grette, 2001; Brigham-Grette & Carter, 1992; Brigham-Grette & Hopkins, 1995). Hopkins (1973, 1982) and others (e.g., Carter, 1993; Péwé, 1975) have identified ancient dunes, shorelines, and wave-cut scarps that can be discontinuously traced across much of the North Slope. A fairly prominent shoreline lies at an elevation of around 23–29 m asl. It has been associated with a pre-Illinois interglacial high stand (Hopkins, 1982; Lewellen, 1972; Sellmann et al., 1975a), and can be traced across the image. This feature demarcates the younger Outer Coastal Plain with surficial marine silts and sands to the north, and the older Inner Coastal Plain with surface aeolian sand to the south (Williams, 1983; Williams et al., 1978).

4. Methods

Landsat-7 data were acquired from the USGS EROS Data Center for the study area. A total of seven Landsat-7 scenes were collected from cloud-free summer months between 2000–2002. The images consisted of Paths 75, 77, and 79 Rows 10 and 11 and Path 81 Row 10. The images were subset using river and coastal boundaries and extended as far south as thaw lakes were present. Images were co-registered to each other and merged following processing (described below) to create a mosaic covering the entire study area (Fig. 1).

4.1. Texture transformation

Thaw lakes and DTLBs have a unique texture that distinguishes them from surrounding vegetation. Thaw lakes have a relatively smooth texture while DTLBs vary in texture according to age. A texture transform was applied to the Landsat-7 dataset to aid in the segmentation and classification of both thaw lakes and DTLBs. Texture measures can be determined from first and second order gray-level statistics (Gong et al., 1992; Haralick, 1986; Hsu, 1978; Irons & Petersen, 1981; Jahne, 1991), Fourier transforms (Gong et al., 1992; Weska et al., 1976), fractal dimension (Lam, 1990; Mandelbrot, 1977, 1982), and stochastic Markov random fields (Dubes & Jain, 1989; Lorette et al., 1998). We used the mean co-occurrence image with an 11×11 window size texture filter of band 5 for input into image segmentation. Co-occurrence measures use a spatial dependence matrix to calculate texture values. The matrix records the frequency with which pixel values occur

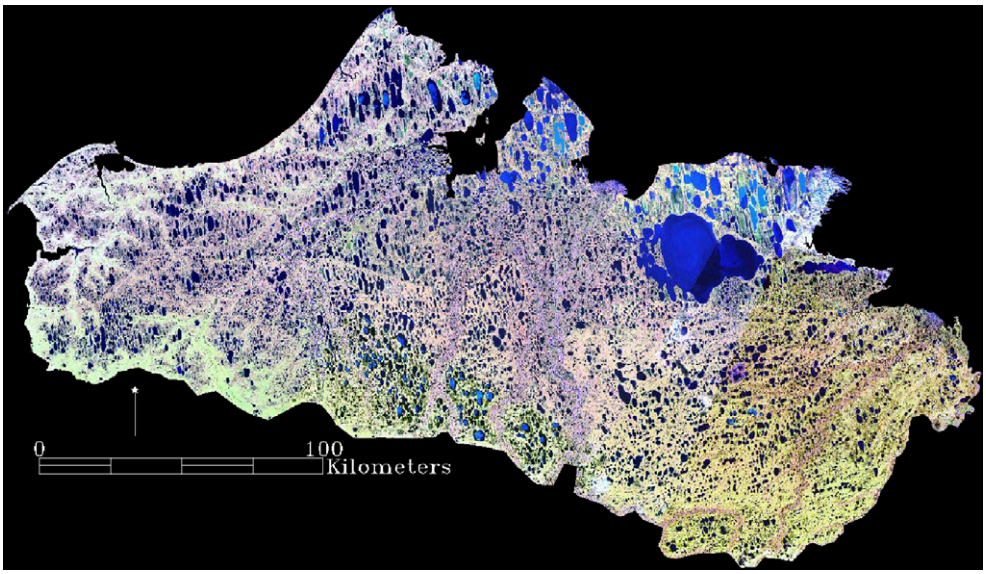

Fig. 1. Mosaic of seven Landsat-7 scenes (bands 543 RGB) showing the study area.

in two neighboring processing windows of a specified size and distance (Haralick, 1986).

4.2. Vegetation transformation

To capture the vegetation component of the Landsat-7 dataset for basin segmentation and classification we applied a Minimum Noise Fraction (MNF) transformation to each scene. The MNF segregates noise in the data, and reduces the computational requirements for further processing (Boardman & Kruse, 1994). The MNF transform consists of two cascaded Principal Component transforms. The first transformation, based on a noise covariance matrix, decorrelates and rescales the noise in the data. The second step is a standard Principal Components transformation of the noise-whitened data (Green et al., 1988). Band 1 of the MNF transformation, which contained primarily near-IR and mid-IR information without the noise in bands 4 and 5, was input for segmentation and classification. Texture and MNF transformations were applied using ENVI 4.0 software from Research Systems, Inc. (www.rsinc.com).

4.3. Image segmentation and classification

Five bands were input for image segmentation and classification from each Landsat-7 scene. Included were bands 3, 4, and 5 of the original data along with MNF band 1 and the mean co-occurrence texture image of band 5. Image segmentation was performed using eCognition® software from Definiens Imaging (www.definiens-imaging.com). The segmentation was a bottom-up region-merging approach starting with single pixel objects. In an optimization pair-wise clustering process, smaller objects were merged into larger objects based on heterogeneity criteria of color and shape. With each iteration, the pair of adjacent objects with the smallest growth from the defined heterogeneity criteria were merged. The process stopped when the smallest growth for merging of adjacent objects exceeded a pre-defined scale parameter. This procedure simulates the simultaneous growth of segments during each step so that output objects are of comparable size and scale (Benz et al., 2004). The heterogeneity criteria considers both spectral and shape properties. Spectral heterogeneity is determined by weighting factors applied to bands used in the segmentation process. Shape heterogeneity is a value that describes the change of the objects shape with respect to smoothness and compactness (Benz et al., 2004). Image segmentation was applied using a scale parameter of 30, a shape factor of 0.10, a compactness of 0.5, and smoothness of 0.5. A total of 82,261 image objects were created from the segmentation of all images. Spectrally similar objects were merged based on scale parameter analysis. The objects were then subjected to a series of membership function decision rules based on spectral, textural, and shape features.

The main feature membership functions used for classification of the thaw lakes were the object mean in band 5 and the object shape values such as shape complexity and elliptic fit. Since both lakes and rivers are water bodies and have similar spectral means, it was necessary to use a shape parameter to distinguish between these two objects in order to classify thaw lakes. An elliptic fit calculation was useful in distinguishing thaw lakes from rivers and streams in the study area. First an ellipse is created with the same area as the considered object. In the ellipse calculation the perimeter to area ratio of the object is used. The area of the object outside the ellipse is compared with the area inside the ellipse and a fit value is calculated for the object. The calculation ranges from zero for no fit to unity, representing a perfect fit to an ellipse. Fig. 2 shows a portion of the study area as an image gray-scaled according to elliptic fit. High elliptic fit values are shown in white and

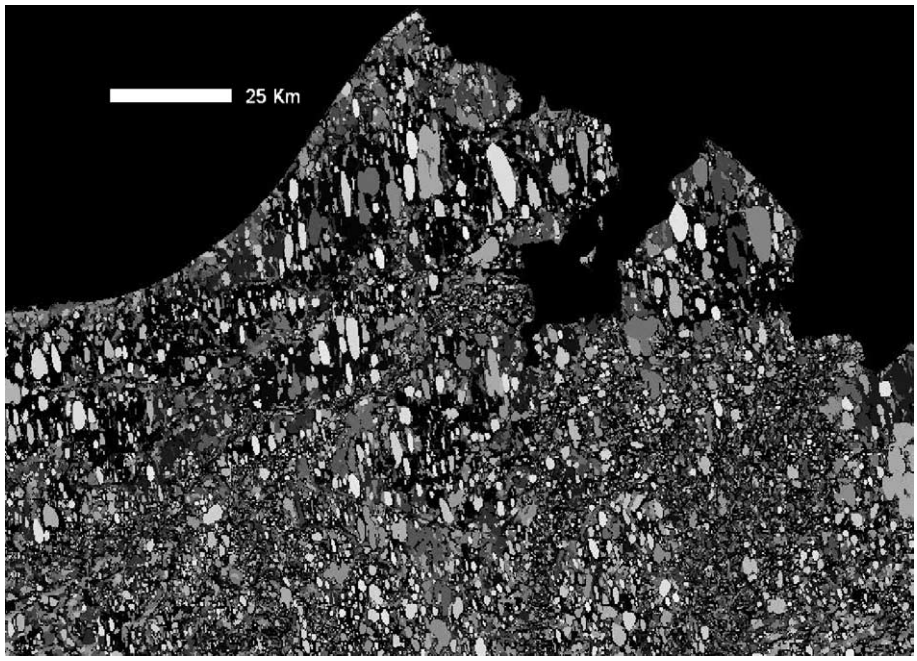

Fig. 2. Image of a portion of the study area for elliptic fit values of image objects gray-scaled from low (black) to high (white) values. Thaw lakes have high elliptic fit values and are brightest in the image.

low values in black; gray values are scaled linearly across the range. Thaw lakes have very high elliptic fit values as the lakes are ellipsoid in shape. By contrast, rivers and streams have very low elliptic fit values. Thaw lakes were extracted from the water object class by use of the elliptic fit and a shape complexity measures.

For classification of DTLBs, membership functions consisted of the spectral means of objects for bands 3, 4, 5 and MNF band 1, as well as the mean co-occurrence and shape complexity values of objects in the final classification. Texture was an important membership function for the classification of DTLBs. Fig. 3 shows texture values for

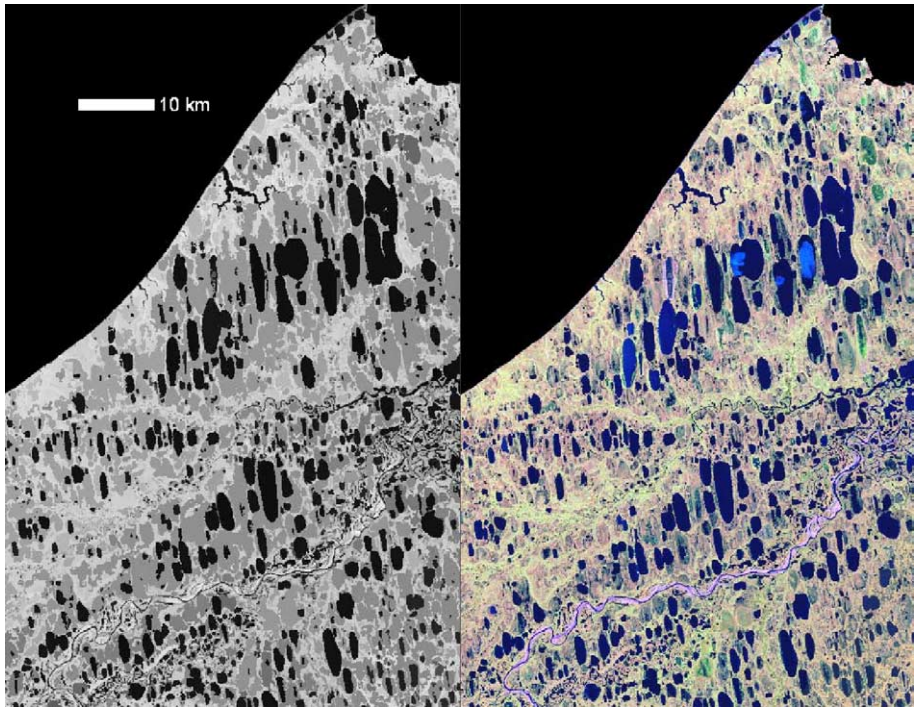

Fig. 3. *Left:* Image of a portion of the study area for the band 5 mean co-occurrence texture values of image objects gray-scaled from smooth (black) to coarse (white). DTLBs have medium texture and high contrast from surrounding vegetation with coarser textures, and from lakes which have smoother textures. *Right*: Landsat-7 composite (543 RGB) of the same area.

Table 1
Contingency matrix for the accuracy assessment of the thaw lake and drained basin classification

Class	Drained basins	Thaw lakes	Other	Total
Drained basins	**256 (93.77)** ***(98.08)***	1 (0.47) *(0.38)*	4 0.78 *(1.53)*	**261**
Thaw lakes	3 (1.10) *(1.41)*	**210 (99.06)** ***(98.59)***	0 (0.0) *(0.0)*	**213**
Other	14 (5.13) *(2.66)*	1 (0.57) *(0.19)*	***511 (99.22)*** ***(97.15)***	**526**
Total	**273**	**212**	**515**	**1000**

The diagonals are pixels correctly classified with producer accuracy **(in parenthesis bold)** and user accuracy ***(in parenthesis bold italics)*** for each class. Non-diagonals represent pixel errors with omission percentage (in parentheses) and commission error percentage *(in parentheses and italics)*.

objects based on mean co-occurrence in band 5. Objects are gray-scaled from smooth texture values (dark objects) to coarse texture values (bright objects). DTLBs are shown in gray tones indicating that these objects have medium texture. These basins have a high contrast from surrounding vegetation which has coarser textures, and from lakes which have much smoother textures. A series of membership function decision rules were applied to all of the remaining objects to get a final classification of each object as thaw lake, DTLB, or "other".

4.4. Accuracy assessment

An accuracy assessment was performed on the thaw lake and drained thaw lake basin classification. A total of 1000 stratified random sample points were identified using photo-interpretation of the Landsat-7 imagery with the aid of IKONOS and Quickbird data, as well as high resolution aerial photographs. It should be noted that thaw lake basins are difficult to identify from the ground because of their shallow gradients; thus the use of aerial photography and satellite imagery is important in identifying their location.

A contingency matrix was constructed to compare the photo-interpreted points to the final classified map. Descriptive statistics were used to evaluate information in each error matrix. Overall accuracy was calculated by dividing the total correct pixels by the total number of pixels in the error matrix. Individual class user and producer accuracies and errors of omission and commission were calculated following Story and Congalton (1986). Kappa coefficient was also calculated to compare the accuracy of the classifications to that of a random pixel classification (Congalton et al., 1983).

5. Results and discussion

The results for the accuracy assessment are shown in Table 1. The overall classification accuracy was 97.7% with a Kappa Coefficient of 0.96. DTLBs had a producer accuracy of 93.8% and user accuracy of 98.1%. Thaw lakes had a producer accuracy of 99.1% and a user accuracy of 98.6%. The main error of omission (5.13%) for DTLBs was confusion with the "other" category. These are mainly basins that the classification missed and were put in the general "other" category (not drained basins or lakes).

The final classification of thaw lakes is shown in Fig. 4. There were a total of 7054 km^2 of thaw lakes mapped, accounting for 20.4% of the study area. This proportion is in agreement with Sellmann et al. (1975a). The final classification of DTLBs is shown in Fig. 5. There were 8917 km^2 of DTLBs mapped, or 25.7% of the study area. A histogram showing the distribution of lakes and DTLBs by size (>1 ha), along with summary statistics, is shown as Fig. 6. The large number of DTLBs exceeding 20 km^2 is likely due to

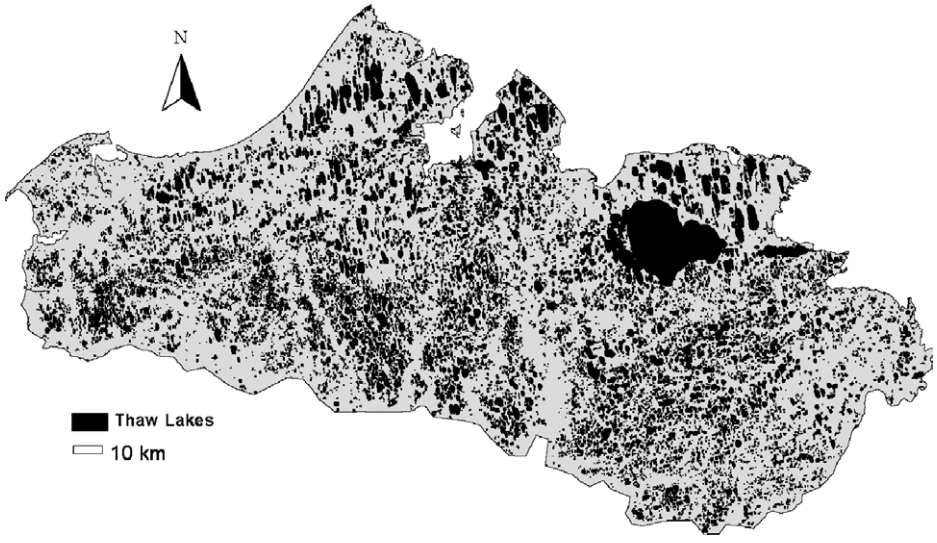

Fig. 4. Final classified map of thaw lakes on the western Arctic Coastal Plain.

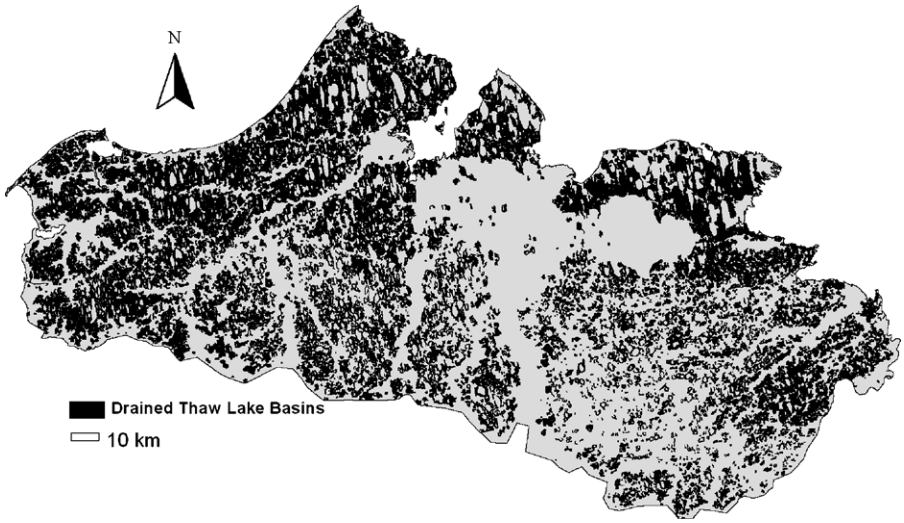

Fig. 5. Final classified map of DTLBs on the western Arctic Coastal Plain.

merging of adjoining basins into a single large complex object.

The orientation of the major axis of both lakes and basins in the study area is shown in Fig. 7. For both datasets, the average orientation differs from the median orientation by ~6°. This likely reflects the influence of the large number of small, non-oriented lakes on the summary parameters. The difference in the orientation of lakes and DTLBs is statistically insignificant.

The combined area of thaw lakes and drained basins covers 46.1% of the entire area of the North Slope of Alaska. This proportion is less than that reported by Hussey and Michaelson (1966) who estimated that 50–75% of the Alaskan Coastal Plain was covered by lakes, marshes, and drained basins. However, Hussey and Michaelson's (1966) estimates were based on analysis of the Barrow Peninsula, at the northernmost part of the maps. This area clearly has much larger thaw lakes and basins.

Fig. 8 shows a zoomed area of the Barrow Peninsula for both the thaw lake and DTLBs classification. Lakes in this area of the Outer Coastal Plain are much larger than the rest of the study area. The largest lake was ~36 km^2 with a major axis length of 12 km. DTLBs are even larger and cover 44.5% of the surface area. Lakes account for 21.5% of the surface area, and combined with DTLBs, cover nearly 66% of the Barrow Peninsula. This proportion is more in line with Hussey's and Michaelson's (1966) estimate of 50–75%. It also corresponds closely to the

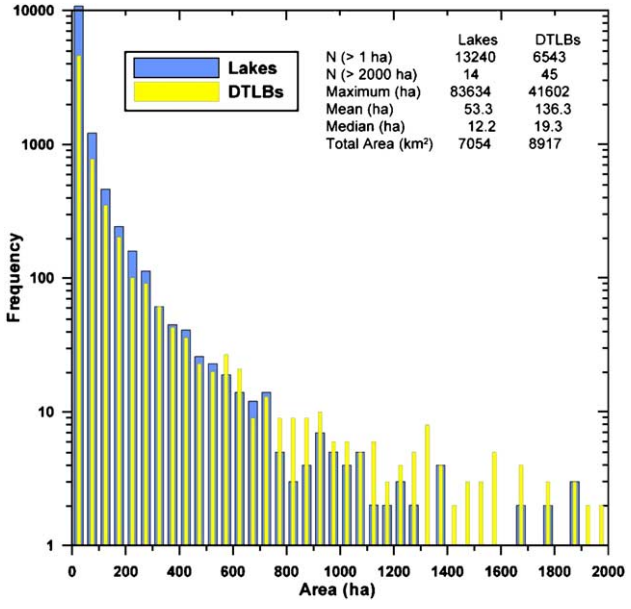

Fig. 6. Histogram of lakes and DTLBs (>1 ha) in entire scene, with summary statistics.

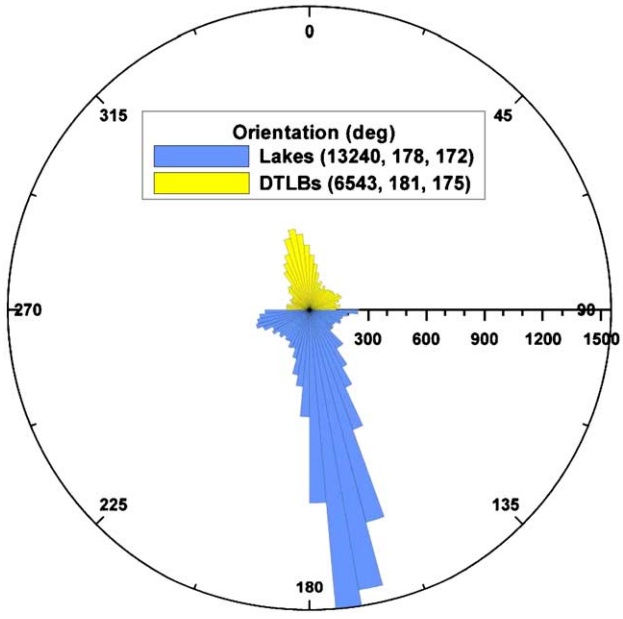

Fig. 7. Orientation of lakes and DTLBs (>1 ha) in entire scene. The numbers in the parentheses represent the number of objects, mean orientation (degrees), and median orientation (degrees).

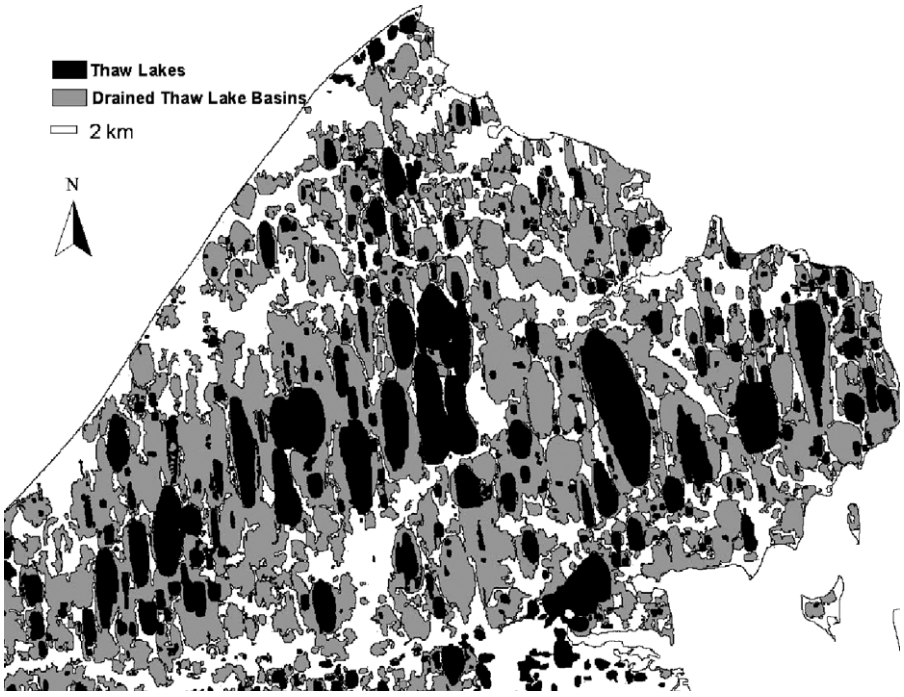

Fig. 8. Zoomed area of the Barrow Peninsula for both the thaw lake and DTLB classification.

results of Hinkel et al. (2003), who report that 22% of the Barrow Peninsula is covered by lakes and at least 50% is scarred by DTLBs. By contrast, Fig. 9 shows a zoomed area of the southeastern portion of the Inner Coastal Plain in the classified map. In this area, thaw lakes and DTLBs are much smaller. The largest lake in this area is 18 km^2

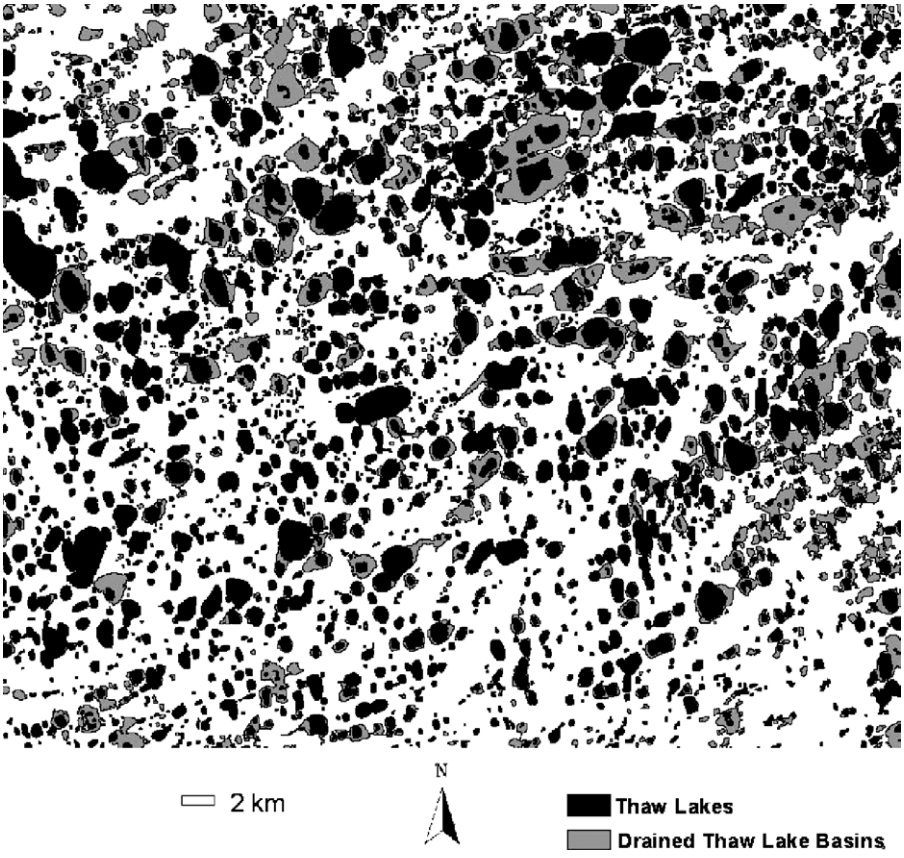

Fig. 9. Zoomed area of the southeastern portion of the Inner Coastal Plain for both the thaw lake and DTLB classification.

with a major axis 7.5 km in length. DTLBs cover 14.1%, and thaw lakes cover 22.1% of the surface area. The combined proportion of thaw lakes and basins in this area is only 36.2% of the total area.

The Outer Coastal Plain in western Alaska is younger than the Inner Coastal Plain and is characterized by larger thaw lakes and greater density of lakes and DTLBs. Sellman et al. (1975a) described the Outer Coastal Plain as having lower relief and lakes that exceed 6 km in length. In our analysis of the Outer Coastal Plain (0–23 m asl) from the lake classification, there were 4809 thaw lakes with an average lake size of 74 ha. On the Inner Coastal Plain there were 8510 lakes with an average lake size of 35 ha. The largest lake in the Outer Coastal Plain (excluding Teshekpuk Lake at 836 km^2) was 58.3 km^2 compared to only 1.8 km^2 for the largest lake on the Inner Coastal Plain. Carson and Hussey (1962) referred to the Outer Coastal Plain as the "Northern Alaska Lake District". They further divided the area into a Western and an Eastern section. They described basins in the western section as subelliptical to subrectangular, with a tendency for large basins near the coast, especially at Point Barrow. A high percentage of basins in the western section were at least 1.5 km in length, with a few as much as 14 km long (Carson & Hussey, 1962). Carson and Hussey (1962) described the eastern section as having basins with the same orientation as those in the western but differing in size and shape. Basins were smaller and more uniform in size in the eastern section with lengths rarely exceeding 1.5 km.

6. Summary and conclusion

There are many advantages to using Landsat-7 data for the analysis of thaw lakes and DTLBs on the North Slope of Alaska. First, the lakes and DTLBs on the North Slope span an areal scale ranging across 5–6 orders of magnitude. Small scale topographic maps do not have the degree of detail necessary to identify and map DTLBs and their complex shapes. The Landsat-7 data allows mapping of spectral and geomorphological features across a range of scales. Second, the spatial and spectral resolution of Landsat-7 is ideal for providing textural, spatial, and spectral patterns to distinguish DTLBs. In many cases, a basin margin cannot be identified from the ground or topographic map, but it is clearly detectable in the image. The spatial extent of the images also covers enough ground area that DTLBs on the western North Slope of Alaska can be mapped with 7–8 scenes. Finally, it is not feasible to sample every basin to collect field measurements of organic layer thickness, thaw depth, and SOC. However, by correlating image parameters with representative DTLB samples, the results can be extrapolated across the entire study area to provide realistic, spatially distributed estimates of soil organic carbon.

To date, field sampling to assess soil carbon stocks have been confined to the Barrow Peninsula. Future studies will focus on lake and DTLB development with respect to different physiographic regions on the North Slope of Alaska. The methodology used in this study could also be applied to other areas with thaw lakes such as Northern Canada and Western Siberia. In a recent paper (Hinkel et al., in press), we utilized the methods described here as the basis for a statistical analysis of metrics describing shape and orientation of lakes and basins across the western Arctic Coastal Plain. Factors that effect lake and DTLB morphometry include the age of the surface, type of surficial sediments, topography, relief and ground ice content. Continued research on primary geomorphic and biochemical processes is essential to our understanding of the global carbon cycle, atmospheric methane concentrations, surface energy balance, and the impacts of global climate change on sensitive environments.

Acknowledgements

This work was supported by the National Science Foundation under grants OPP-9911122 and 0240174 to WRE, and OPP-9732051 and 0094769 to KMH. Any opinions, findings, conclusions, or recommendations expressed in this material are those of the authors and do not necessarily reflect the views of the National Science Foundation. We are grateful for logistical support from the Barrow Arctic Science Consortium and the Ukpeagvik Inupiat Corporation.

References

Benz, U. C., Hofmann, P., Willhauck, G., Lingenfelder, I., & Hetnen, M. (2004). Multi-resolution, object-oriented fuzzy analysis of remote sensing data for GIS-ready information. *ISPRS Journal of Photogrammetry and Remote Sensing*, *58*, 239–258.

Billings, W. D., & Peterson, K. M. (1980). Vegetational change and ice-wedge polygons through the thaw-lake cycle in Arctic Alaska. *Arctic and Alpine Research*, *1*, 413–432.

Billings, W. D., Luken, J. O., Mortensen, D. A., & Peterson, K. M. (1982). Arctic tundra: A source or sink for atmospheric carbon dioxide in a changing environment? *Oecologia*, *58*, 286–289.

Black, R. F. (1969). Thaw depressions and thaw lakes–a review. *Biuletyn Peryglacjalny*, *19*, 131–150.

Bliss, L. C., & Peterson, K. M. (1992). Plant succession, competition, and the physiological constraints of species in the arctic. In F. S. Chapin, R. L. Jefferies, J. F. Reynolds, G. R. Shaver, & J. Svoboda (Eds.), *Arctic ecosystems in a changing climate: An ecophysiological perspective* (pp. 111–136). San Diego, CA: Academic Press.

Boardman, J. W., & Kruse, F. A. (1994). Automated spectral analysis: A geological example using AVIRIS data, north Grapevine Mountains Nevada. *Proceedings, ERIM tenth thematic conference on geologic remote sensing* (pp. I-407–I-418). Ann Arbor, MI: Environmental Research Institute of Michigan.

Bockheim, J. G., Hinkel, K. M., Eisner, W. R., Dai, X. Y., & Peterson, K. M. (2004). Carbon pools and accumulation rates in an age-series of soils in drained thaw-lake basins, Arctic Alaska. *Soil Science Society of America Journal*, *68*, 697–704.

Brigham-Grette, J. (2001). New perspectives on Beringian Quaternary paleogeography, stratigraphy, and glacial history. *Quaternary Science Reviews*, *20*, 15–24.

Brigham-Grette, J., & Carter, L. D. (1992). Pliocene marine transgressions of northern Alaska: Circumarctic correlations and paleoclimate interpretations. *Arctic*, *45*, 74–89.

Brigham-Grette, J., & Hopkins, D. (1995). Emergent marine record and paleoclimate of the last interglaciation along the Northwest Alaskan Coast. *Quaternary Research*, *43*, 159–173.

Britton, M. E. (1966). Vegetation of the Arctic tundra. In H. P. Hansen (Ed.), *Arctic Biology* (pp. 26–61). Corvallis: Oregon State University.

Carson, C. E., & Hussey, K. M. (1962). The oriented lakes of Arctic Alaska. *Journal of Geology*, *60*, 417–439.

Carter, L. D. (1993). Late Pleistocene stabilization and reactivation of eolian sand in northern Alaska: Implications for the effects of future climatic warming on an eolian landscape in continuous permafrost. *Proceedings of the sixth international conference on permafrost* (pp. 78–83). Wushan Guangzhou, China: South China University of Technology Press.

Christensen, T. R., Johansson, T., Akerman, J. G., Mastepanov, M., Malmer, N., Friborg, T., et al. (2004). Thawing sub-arctic permafrost: Effects on vegetation and methane emissions. *Geophysical Research Letters*, *31*, L04501.

Congalton, R. G., Oderwald, R. G., & Mead, R. A. (1983). Assessing landsat classification accuracy using discrete multivariate statistical techniques. *Photogrammetric Engineering and Remote Sensing*, *49*(12), 1671–1678.

Côté, M. M., & Burn, C. R. (2002). The oriented lakes of Tuktoyaktuk Peninsula, Western Arctic Coast, Canada: A GIS-based analysis. *Permafrost and Periglacial Processes*, *13*, 61–70.

Dubes, R. C., & Jain, A. K. (1989). Random fields models in image analysis. *Journal of Applied Statistics*, *16*, 2.

Eisner, W. R., & Peterson, K. M. (1998). Pollen, fungi and algae as age indicators of drained lake basins near Barrow, Alaska. In A. G. Lewkowicz, & M. Allard (Eds.), *7th international conference on Permafrost, Yellowknife, Canada* (pp. 245–250). Laval, Quebec: Centre de etudes nordiques de l'Universite Laval.

Eisner, W. R., Bockheim, J. G., Hinkel, K. M., Brown, T. A., Nelson, F. E., Peterson, K. M., et al. (2005). Paleoenvironmental analyses of an organic deposit from an erosional landscape remnant, Arctic Coastal Plain of Alaska. *Paleogeography, Paleoclimatology, Paleoecology*, *217*, 187–204.

Frohn, R. C., Eisner, W. R., Hinkel, K. M., & Arellano-Neri, O. (2001). Remote sensing of thaw lake basins on the North Slope of Alaska. *Proceedings American society of photogrammetry and remote sensing on CD-ROM*.

Gong, P., Marceau, D. J., & Howarth, P. J. (1992). A comparison of spatial feature extraction algorithms for land-use classification with SPOT HRV data. *Remote Sensing of Environment*, *40*, 137–151.

Green, A. A., Berman, M., Switzer, P., & Craig, M. D. (1988). A transformation for ordering multispectral data in terms of image quality with implications for noise removal. *IEEE Transactions on Geoscience and Remote Sensing*, *26*, 65–74.

Haralick, R. M. (1986). Statistical image texture analysis. In T. Y. Young, & K. S. Fu (Eds.), *Hand-book of pattern recognition and image processing* (pp. 247–280). New York: Academic Press.

Hinkel, K. M., Eisner, W. R., Bockheim, J. G., Nelson, F. E., Peterson, K. M., & Dai, X. (2003). Spatial extent, age, and carbon stocks in drained thaw lake basins at the Barrow Peninsula. *Alaska, Arctic, Antarctic, and Alpine Research*, *35*, 291–300.

Hinkel, K. M., Frohn, R. C., Nelson, F. E., Eisner, W. R., & Beck, R. A. (in press). Morphometric and spatial analysis of thaw lakes and drained thaw lake basins in the western Arctic Coastal Plain, Alaska. *Permafrost and Periglacial Processes*, *16*.

Hopkins, D. M. (1949). Thaw lakes and thaw sinks in the Imuruk Lake area, Seward Peninsula. *Journal of Geology*, *57*, 119–131.

Hopkins, D. M. (1973). Sea level history in Beringia during the last 210,000 years. *Quaternary Research*, *3*, 520–540.

Hopkins, D. M. (1982). Aspects of the paleogeography of Beringia during the late Pleistocene. In D. M. Hopkins, J. V. Matthews, Jr., C. E. Schweger, & S. B. Young (Eds.), *Paleogeography of Beringia* (pp. 3–28). New York: Academic Press.

Hopkins, D. M., & Kidd, J. G. (1988). Thaw lake sediments and sedimentary environments. *Permafrost 5th international conference* (pp. 3–28). Trondheim: Tapir Publishers.

Hsu, S. (1978). Texture-tone analysis for automated landuse mapping. *Photogrammetric Engineering and Remote Sensing*, *44*, 1393–1404.

Hussey, K. M., & Michelson, R. W. (1966). Tundra relief features near Point Barrow, Alaska. *Arctic*, *19*, 162–184.

Irons, J. R., & Petersen, G. W. (1981). Texture transforms of remote sensing data. *Remote Sensing of Environment*, *11*, 359–370.

Jahne, B. (1991). *Digital image processing*. New York: Springer-Verlag. 383 pp.

Jeffries, M. O., Morris, K., & Liston, G. E. (1996). A method to determine lake depth and water availability on the North Slope of Alaska with spaceborne imaging radar and numerical ice growth modeling. *Arctic*, *49*, 367–374.

Jeffries, M. O., Zhang, T., Frey, K., & Kozlenko, N. (1999). Estimating late-winter heat flow to the atmosphere from the lake-dominated Alaskan North Slope. *Journal of Glaciology*, *45*, 315–324.

Kane, D. L., Hinzman, L. D., Woo, M.-k., & Everett, K. R. (1992). Arctic hydrology and climate change. In F.S.I.I.I. Chapin, R. L. Jefferies, J. F. Reynolds, G. R. Shaver, & J. Svoboda (Eds.), *Arctic ecosystems in a changing climate: An ecophysiological pespective* (pp. 35–57). San Diego: Academic Press.

Kozlenko, N., & Jeffries, M. O. (2000). Bathymetric mapping of shallow water in thaw lakes on the North Slope of Alaska with spaceborne imaging radar. *Arctic*, *53*, 306–316.

Lam, N. S. (1990). Description and measurement of landsat TM images using fractals. *Photogrammetric Engineering and Remote Sensing*, *56*(2), 187–195.

Lewellen, R. I. (1972). *Studies on fluvial environment, Arctic Coastal Plain Province, Northern Alaska*. Littleton, CO: Author.

Livingstone, D. A., Bryan, K., & Leahy, R. G. (1958). Effects of an arctic environment on the origin and development of fresh-water lakes. *Limnology and Oceanography*, *3*, 192–214.

Lorette, A., Descombes, X., & Zerubia, J. (1998). Urban areas extraction based on markovian modelling. *Research Center INRIA Report*.

Mackay, J. R. (1988). Catastrophic Lake Drainage, Tuktoyaktuk Peninsula area, District of Mackenzie. Current Research, Part D, Geological Survey Can. *Paper*, *88-1D*, 83–90.

Mackay, J. R. (1992). Lake stability in an ice-rich permafrost environment: Examples from the western Arctic coast. In R. D. Robarts, & M. L. Bothwell (Eds.), *Aquatic ecosystems in semi-arid regions: Implications for resource management*, *vol. 7* (pp. 1–25). Saskatoon: Environment Canada.

Mackay, J. R., & Burn, C. R. (2002). The first 20 years (1978–1979 to 1998–1999) of ice-wedge growth at the Illisarvik experimental drained lake site, western Arctic coast, Canada. *Canadian Journal of Earth Sciences*, *39*(1), 95–111.

Mandelbrot, B. B. (1977). *Fractals: Form, chance, and dimension*. San Francisco: W. H. Freeman.

Mandelbrot, B. B. (1982). *The fractal geometry of nature*. San Francisco: W. H. Freeman.

Mellor, J. C. (1994). ERS-1 SAR use to determine lake depths in arctic and subarctic regions. *Proceedings of the Second ERS-1 Symposium, Hamburg* (pp. 1141–1146).

Péwé, T. L. (1975). Quaternary geology of Alaska. *USGS Professional Paper*, *835*.

Phelps, A. R., Peterson, K., & Jeffries, M. O. (1998). Methane efflux from high latitude lakes during spring ice-melt. *Journal of Geophysical Research*, *103*, 29029–29036.

Sellmann, P. V., Brown, J., Lewellen, R. I., McKim, H., Merry, C. (1975a). The classification and geomorphic implications of thaw lakes on the Arctic coastal plain, Alaska:. US Army CRREL Research Report, 344: 21.

Sellman, P. V., Weeks, W. F. & Campbell, W. J. (1975b). Use of sidelooking airborne radar to determine lake depth on the Alaskan North Slope. Special Report 230, Hanover, New Hampshire. U.S Army Cold Regions Research and Engineering Laboratory.

Serreze, M. C., Walsh, J. E., Chapin III, F. S., Osterkamp, T., Dyurgerov, M., Romanovsky, V., et al. (2000). Observational evidence of recent change in the northern high latitude environment. *Climatic Change*, *46*, 159–207.

Smith, L. C., MacDonald, G. M., Velichko, A. A., Beilman, D. W., Borisova, O. K., & Frey, K. E., et al. (2004). Siberian peatlands a net carbon sink and global methane source since the early Holocene. *Science*, *303*, 353–356.

Story, M., & Congalton, R. (1986). Accuracy assessment: A user's perspective. *Photogrammetric Engineering and Remote Sensing*, *52*, 397–399.

Waelbroeck, C., Monfray, P., Oechel, W. C., Hastings, S., & Vourlitis, G. (1997). The impact of permafrost thawing on the carbon dynamics of tundra. *Geophysical Research Letters*, *24*(3), 229–232.

Wahrhaftig, C. (1965). Physiographic Divisions of Alaska. *USGS Professional Paper*, *482*.

Walker, H. J. (1978). Lake tapping in the Colville River Delta. *3rd International conference on permafrost, Ottawa*. National Research Council of Canada, Publishing.

Webber, P. J. (1978). Spatial and temporal variation of the vegetation and its production, Barrow, Alaska. In L. L. Tieszen (Ed.), *Vegetation and production ecology of an Alaskan Arctic Tundra* (pp. 37–112). New York: Springer Verlag.

Weller, G., Chapin, F. S., Everett, K. R., Hobbie, J. E., Kane, D., Oechel, W. C., et al. (1995). The arctic flux study: A regional view of trace gas release. *Journal of Biogeography*, *22*, 365–374.

Weska, J., Dyer, C., & Rosenfeld, A. (1976). A comparative study of texture measures for terrain classification. *IEEE Transactions on Systems, Man, and Cybernetics*, *6*, 269–285.

Williams, J. R. (1983). Engineering-geologic maps of northern Alaska, Meade river quadrangle. *U.S. Geological Survey Open-File*, 83–294.

Williams, J. R., Carter, L. D., & Yeend, W. E. (1978). Coastal plain deposits of NPRA. B20-22. In K. M. Johnson (Ed.), *The United States geological survey in Alaska: Accomplishments during 1977* (pp. 772-B). GS Circular.